
This is an electronic reprint of the original article.
This reprint may differ from the original in pagination and typographic detail.

Kyosti, Pekka; De Guzman, Mar Francis; Haneda, Katsuyuki; Tervo, Nuutti; Parssinen, Aarno
How many beams does sub-THz channel support

Published in:
IEEE Antennas and Wireless Propagation Letters

DOI:
[10.1109/LAWP.2021.3118464](https://doi.org/10.1109/LAWP.2021.3118464)

Published: 01/01/2022

Document Version
Publisher's PDF, also known as Version of record

Published under the following license:
CC BY

Please cite the original version:
Kyosti, P., De Guzman, M. F., Haneda, K., Tervo, N., & Parssinen, A. (2022). How many beams does sub-THz channel support. *IEEE Antennas and Wireless Propagation Letters*, 21(1), 74-78.
<https://doi.org/10.1109/LAWP.2021.3118464>

This material is protected by copyright and other intellectual property rights, and duplication or sale of all or part of any of the repository collections is not permitted, except that material may be duplicated by you for your research use or educational purposes in electronic or print form. You must obtain permission for any other use. Electronic or print copies may not be offered, whether for sale or otherwise to anyone who is not an authorised user.

How Many Beams Does Sub-THz Channel Support?

Pekka Kyösti , Mar Francis De Guzman , Katsuyuki Haneda , *Member, IEEE*,
Nuutti Tervo , *Graduate Student Member, IEEE*, and Aarno Pärssinen 

Abstract—Antenna, radio frequency (RF) circuit, algorithm, and system researchers on sub-THz RF are interested in knowing characteristics of corresponding radio channels. Among other things, a relevant question is the number of beams supported by the channel. From wideband directional propagation measurements one can estimate how many significant paths are present in a measurement location, but interpreting that to separable beams is not trivial. In this letter, we introduce three methods to approximate the number of beams that a measured power angular delay profile can support. We show also example evaluations and distribution functions of beam numbers, estimated from indoor D-band measurement data.

Index Terms—Beam, measurements, propagation, terahertz.

I. INTRODUCTION

SUB-THz or better defined as upper millimeter-wave (mm-wave) frequency region, i.e., 100–300 GHz, is highly interesting for communications and positioning research aiming at future sixth-generation (6G) networks [1]. Extremely directive antennas are a necessity to compensate for severe propagation losses and maintain decent signal to noise power ratio (SNR) with potentially very wide signal bandwidths [2].

Antenna, RF hardware (HW), algorithm, and system researchers must know typical characteristics of sub-THz radio propagation. For example, the following questions are set and wait for answers. Is line of sight (LOS) the only path that has enough gain to conduct communication or positioning signals? Do antenna arrays, related phase control circuits, and/or lenses, need capability for multiple simultaneous beams or is only one sufficient? Is spatial multiplexing a viable option? Are there spare beam directions available if the LOS path is temporally blocked? Some recent work has given analysis for a specific case related to 5G including also RF nonidealities [3].

The mentioned need has led to increasing activity in channel measurements in sub-THz and THz frequencies. Unidirectional and bidirectional multipath propagation measurements have

been reported, covering azimuth only [4], [5] or also including elevation [6]. Joint power angular delay profiles (PADPs) typically collected by such measurements are sufficient for beam evaluations introduced in Section II.

In conventional multiantenna radios, the number of independent beams has been analyzed in the context of spatial diversity and multiplexing. They are defined by the number of *eigenchannels* whose gain is greater than the noise level. They depend on the antenna geometry and wave propagation conditions. The upper limit of the number of eigenchannels is called degrees-of-freedom [7], [8]. It was shown that the degrees-of-freedom do not decrease in the lower mm-wave band even if the RF increases, as far as the physical antenna aperture size remains constant [9].

Phased antenna arrays have been regarded as a realization of antenna arrays at mm-wave and Terahertz radios. The number of RF chains is expected to be much smaller than that of antenna elements [10]. While phased antenna array designs usually aim at forming beams with a clear peak gain to specific directions, e.g., [11], such beams have different shapes from those of eigenchannels, i.e., *eigenbeamforming*, and hence are suboptimal from the channel capacity maximization perspective [12]. For example, for a multiantenna transceiver with a single RF chain, the optimum antenna weight is known to be maximum ratio combining. Its realized beam pattern does not have the same shape as that with a clear peak gain to a specific direction when there are multipaths in the channel. It has been reported that mm-wave and Terahertz channels have ample multipaths [4]–[6].

The present letter discusses the number of independent beams of upper mm-wave indoor channels from the phased antenna array instead of eigen beam forming perspectives, because of its popularity at the frequency band. The derived number of beams is thought of a practical upper limit of the number of independent beams, while it is always smaller than the degrees-of-freedom of the channel.

II. PAS EVALUATION METHODS

The starting point is noise cut measurement data providing powers, delays, and azimuth angles of discrete multipaths in different environments and transmitter (Tx) and receiver (Rx) locations. The Tx and Rx have fixed spatial positions denoted by index $q = 1, \dots, Q$. At this point, we assume angle of arrival (AoA) estimates from Rx. The PADP of link q is $P_q(\Omega, \tau)$. With discrete measurement data, having quantized delay and angle parameters, it is a finite sum

$$P_q(\Omega, \tau) = \sum_{l=1}^{L_q} P_{l,q} \delta(\Omega - \Omega_{l,q}) \delta(\tau - \tau_{l,q}) \quad (1)$$

Manuscript received September 25, 2021; accepted October 2, 2021. Date of publication October 7, 2021; date of current version January 12, 2022. This work was supported in part by the European Commission through the H2020 Project Hexa-X under Grant 101015956 and in part by 6G Flagship programme, funded by Academy of Finland under Grant 318927. (*Corresponding author: Pekka Kyösti.*)

Pekka Kyösti is with the Centre for Wireless Communications, University of Oulu, 90570 Oulu, Finland, and also with Keysight Technologies Finland Oy, 90630 Oulu, Finland (e-mail: pekka.kyosti@oulu.fi).

Mar Francis De Guzman and Katsuyuki Haneda are with the School of Electrical Engineering, Aalto University, 90630 Espoo, Finland (e-mail: francis.deguzman@aalto.fi; katsuyuki.haneda@aalto.fi).

Nuutti Tervo and Aarno Pärssinen are with the Centre for Wireless Communications, University of Oulu, 90570 Oulu, Finland (e-mail: nuutti.tervo@oulu.fi; aarno.parssinen@oulu.fi).

Digital Object Identifier 10.1109/LAWP.2021.3118464

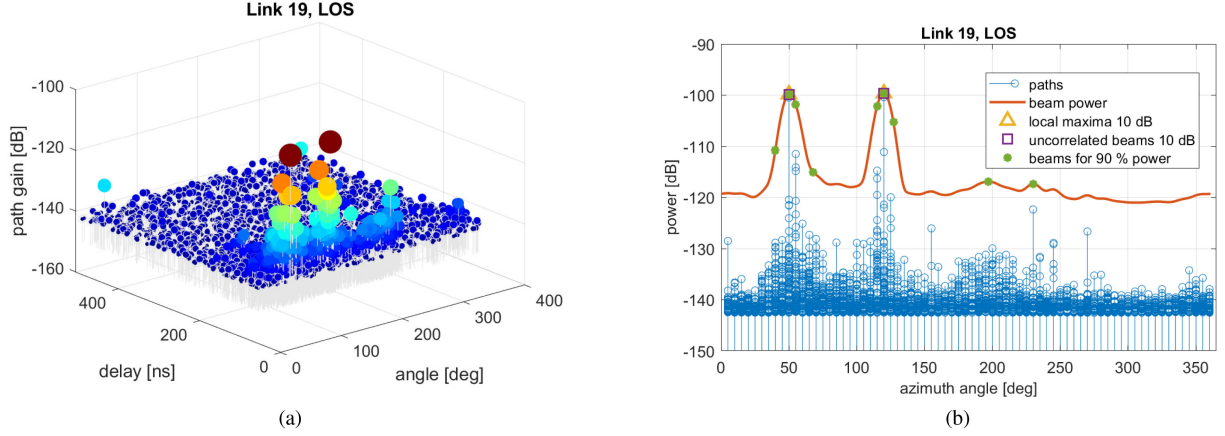


Fig. 1. (a) PADP $P_{19}(\Omega, \tau)$ of link number 19. (b) Path powers, beam power $B_{19}(\alpha)$, and selected beam directions with different methods. Link 19 corresponds to Airport Rx1/Tx1, LOS AoA = 52° in [14].

where L_q is the number of paths, $\delta(\cdot)$ is the delta function, and $P_{l,q}$, $\Omega_{l,q}$, and $\tau_{l,q}$ are the gain (squared magnitude), angle, and propagation delay of the l th path of link q , respectively. An example of measured PADP is shown in Fig. 1(a).

Before performing any quantitative assessments on beam numbers, we must define the beam. It is done by specifying a gain pattern $G(\Omega)$. Here, we would need a representative beam pattern at the considered sub-THz frequencies. It can be either a steered beam of a representative phased array or a beam of a representative directive antenna system. In this letter, we chose a synthetic radiation pattern specified by the third-generation partnership project (3GPP) in [13, Table 7.3-1]. The peak to minimum gain ratio is 30 dB and the definable half-power beamwidth (HPBW) is chosen to be 10° . In general, the angular resolution of the considered beam should not exceed that of the measurement system used for acquiring the data.

In Sections II-A to II-C, we define three alternative methods to evaluate the number of beams supported by propagation channel.

A. Method 1: Number of Local Maxima

The first step is to define the discrete power angular spectrum (PAS) of propagation channel as $P_q(\Omega) = \int P_q(\Omega, \tau) d\tau$. Then, we take convolution of the propagation channel PAS $P_q(\Omega)$ and the beam pattern $G(\Omega)$. This corresponds to steering the beam to all directions α and collecting the sum gain per steering angle. The resulting continuous PAS is

$$B_q(\alpha) = \int P_q(\Omega) G(\alpha - \Omega) d\Omega = \sum_{l=1}^{L_q} P_{l,q} G(\alpha - \Omega_{l,q}). \quad (2)$$

Now, the number of beams on link q is the number of local maxima of function $B_q(\alpha)$ that are within certain dynamic range, i.e., less than X dB below the global maximum of $B_q(\alpha)$. The dynamic range X is a parameter to be set for this evaluation. In this work, we show results using 10 and 20 dB values. The setting depends on communication systems related aspects, e.g., on the target SNR as well as the RF hardware capabilities [3].

The method of local maxima is simple and somewhat intuitive. However, it may lead to less optimal conclusions in specific cases. Some degrees of freedom of the propagation channel

might be lost if, e.g., the paths are grouped in angular domain such that the beam steered PAS $B_q(\alpha)$ yields a wide lobe with a single local maximum only. There is an example of 40° wide path concentration around 90° azimuth with only a single local maximum in Fig. 2(b). Therefore, we propose also another, slightly more complex method in Section II-B, that considers path delays too.

B. Method 2: Number of Uncorrelated Beams

In this method, we extrapolate the original multipath data to artificial impulse responses by introducing a random phase term for each propagation path. The complex directional impulse response of the propagation channel of link q is

$$a_q(\Omega, \tau) = \sum_{l=1}^{L_q} \sqrt{P_{l,q}} e^{i\psi_{l,q}} \delta(\Omega - \Omega_{l,q}) \delta(\tau - \tau_{l,q}) \quad (3)$$

where $i^2 = -1$ and the phase term $\psi_{l,q} \sim \text{Uni}(0, 2\pi)$. Then, we perform beam steering and get complex impulse responses per steering angle α as

$$\begin{aligned} h_q(\alpha, \tau) &= \int a_q(\Omega, \tau) \sqrt{G(\alpha - \Omega)} d\Omega \\ &= \sum_{l=1}^{L_q} \sqrt{P_{l,q} G(\alpha - \Omega_{l,q})} e^{i\psi_{l,q}} \delta(\tau - \tau_{l,q}). \end{aligned} \quad (4)$$

Next, we convert these impulse responses to frequency responses $H_q(\alpha, f)$ using the Fourier transformation. The frequency points f must be specified based on the considered centre frequency, bandwidth, and sample spacing. The correlation coefficient of frequency responses in beam steering angles α_1 and α_2 is

$$R_q(\alpha_1, \alpha_2) = \frac{|\int H_q(\alpha_1, f) \bar{H}_q(\alpha_2, f) df|}{\sqrt{\int |H_q(\alpha_1, f)|^2 df \int |H_q(\alpha_2, f)|^2 df}} \quad (5)$$

where $\bar{(\cdot)}$ is the complex conjugate operator.

For the search algorithm, we must choose a discrete set of beam steering angles. It can be, e.g., from 0° to 359° with one degree spacing. Gain (squared magnitude) $B_q(\alpha)$ and correlations $R_q(\alpha_1, \alpha_2)$ are determined for the selected set of angles α . With Method 2, we must choose one more parameter in addition to the beam pattern and dynamic range that were introduced

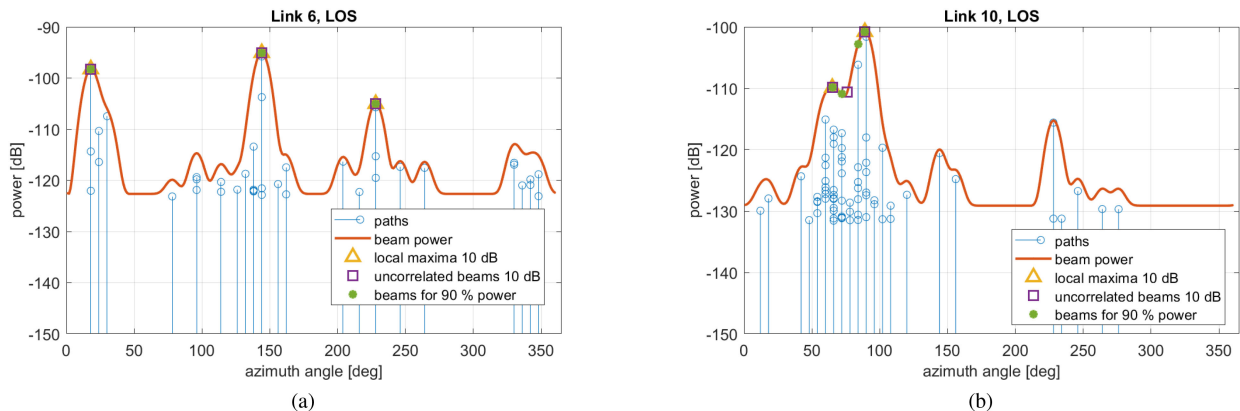


Fig. 2. Path powers, beam power $B_q(\alpha)$, and selected beam directions with different methods in (a) link 6 (b) and link 10. Link 6 corresponds to Rx1/Tx12, LOS AoA = 127° and link 10 Rx1/Tx16, LOS AoA = 183° in [5].

in Method 1 and the aforementioned frequency points. The parameter is the threshold value of correlation coefficient, i.e., the level of acceptable correlation between frequency responses of beams. Let us define empty set $\Gamma = \emptyset$ of beam directions. The algorithm to find uncorrelated beam directions is as follows.

- 1) Find the steering angle α_m that provides maximum B_q and attach it to set Γ of uncorrelated beam directions.
- 2) Find all steering angles α that have correlation above a certain threshold, i.e., $R_q(\alpha_m, \alpha) > \text{threshold}$. Remove those steering angles and corresponding $B_q(\alpha)$.
- 3) Go back to 1), and repeat until all steering angles have been removed. Now the set Γ of uncorrelated beam directions is complete.
- 4) Discard those uncorrelated beam direction whose gain $B_q(\alpha)$ is not within the target dynamic range and remove them from Γ .
- 5) Output is the set Γ of uncorrelated beam directions whose beam gains are within the target dynamic range.

This method considers also propagation delays, instead of mere PAS. If there are numerous paths grouped in an angular sector, Method 2 finds beam directions also outside of the local maxima of B_q . An example of this condition is shown in Fig. 2(b). The assumption of independent random phases across multipaths is reasonable at sub-THz, since the wavelength is very short and even a small displacement changes phases substantially.

C. Method 3: The Minimum Number of Beams for X% Power

This method is slightly different to the previous two. Here, we search for the minimum number of beams that can capture a certain percentage of power available in the propagation channel.¹ The method resembles diversity schemes, where received SNR is maximized using degrees of freedom offered by the channel. The gain pattern is normalized to maximum value of unity as $G'(\alpha) = G(\alpha) / \max \{G(\alpha') | \alpha' \in [0, 2\pi]\}$. Steps of the algorithm are as follows.

- 1) Denote original (squared magnitude) path gains as $P_{l,q}^{\text{prev}}$ and define the empty set $\Gamma = \emptyset$.
- 2) Find the steering angle α_m that provides maximum B_q , attach it to the set Γ of selected beam directions and accumulate the total collected power $\sum_{\alpha \in \Gamma} B_q(\alpha)$.
- 3) Subtract the power captured by the beam from the path powers, i.e., determine new path powers $P_{l,q}^{\text{new}} = P_{l,q}^{\text{prev}} - G'(\alpha_m - \Omega_{l,q}) P_{l,q}^{\text{prev}}$ for all $l \in L_q$.
- 4) Recompute beam power of (2) for all steering angles α with the new path gains.
- 5) Go back to 2) if the accumulated beam power of selected directions is below the target percentage. Otherwise the set Γ of selected beam directions is complete.

Note, in this algorithm all gain/power values are in linear units. With this method, we do not specify the target dynamic range of beam powers. Instead the percentage of power to be collected must be specified. In this letter, we set it to be 90%.

III. RESULTS

In this section, we show beam number analysis results of D-band measurement data provided by Aalto University. Measurements were performed in a shopping mall, an airport, and an entrance hall at approximately 140 GHz. Measurement data contains in total 55 links in the three environments. The propagation condition is either LOS or obstructed line of sight (OLOS). OLOS links are denoted in Fig. 3(a) by blue circle. All components of PADP whose Rx power was below a certain threshold level above the noise level were cut out. Detailed description of the measurements and data is given in [5].

A. Per Link Results

The three methods are applied to measured PADPs to evaluate the number of beams supported by each of 55 links. The following parameters were used on methods. HPBW is 10° , dynamic range either 10 or 20 dB, correlation threshold 0.5, and the target power percentage is 90%. Moreover, the considered frequency band in Method 2 has centre frequency 143 GHz, bandwidth of 2 GHz, and frequency sample spacing of 1 MHz.

¹ Assuming omnidirectional antenna in the other link end. Moreover, not being interested in the absolute power in Watt, we can assume unity transmit power and use received power and channel gain interchangeably.

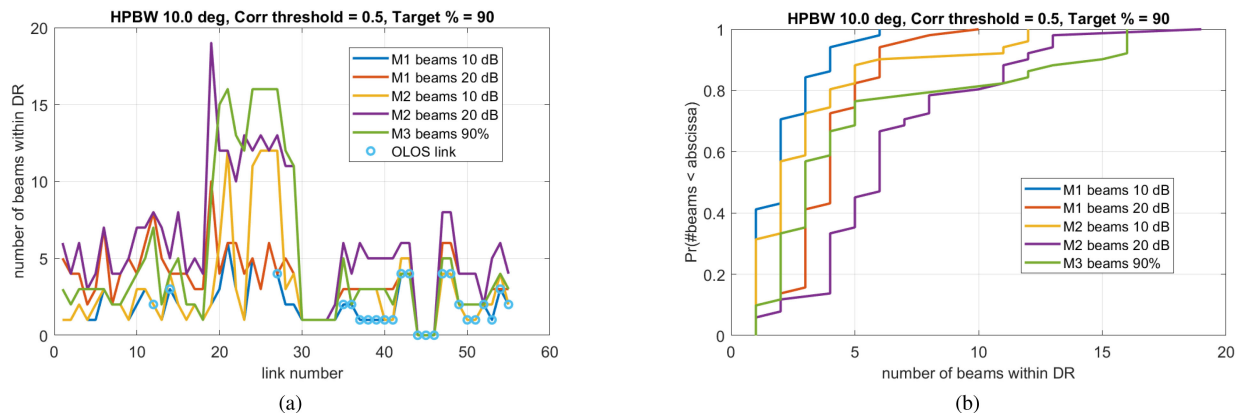


Fig. 3. (a) Number of beams in 55 independent links as determined using three methods and two dynamic range values. (b) Cumulative distribution functions of beam numbers in 55 links using three methods and two dynamic range values.

Beam gains $B_q(\alpha)$ for three LOS links are shown in Figs. 1(b) and 2. Also selected beam directions are shown in the same figures. Methods 1, 2, and 3 are denoted with yellow triangle, violet square, and green star, respectively. In link number six in Fig. 2(a) the beam selection is evident and all methods choose the same three beam directions. This is not the case in figures illustrating $B_q(\alpha)$ of other links. In Fig. 1 there is low gain scattering distributed in all direction with only two significant cluster directions. In this case, Methods 1 and 2 find the same two beam directions, while Method 3 yields seven more beam directions to collect the target 90% of power. In Fig. 2(b), a notable portion of path gains is distributed over a sector of approximately 40° wide, but $B_{10}(\alpha)$ has only two local maxima within the sector. Consequently, Method 1 finds only two prominent beam direction, while 2 and 3 indicate three and four directions, respectively.

B. Distribution of Beam Numbers

In this section, we collect beam numbers over all 55 links and show their distributions. The number of beams identified using the three methods, labeled in the figure as M1...M3, and two dynamic ranges, are illustrated in Fig. 3(a). This is shown as a function of the link identification number. We can remark that Methods 1 and 2 provide similar beam numbers with the dynamic range of 10 dB, except on links supporting highest numbers of beams. In these cases, when the gains are widely dispersed in angular domain, the local maxima method tends to yield lower number of beams. This is understandable observing the example cases of Section III-A.

Corresponding cumulative distribution functions (CDFs) are depicted in Fig. 3(b). The three links, number 44–46, that contained no significant propagation paths and resulted in zero beams, are removed from the CDFs. The median value on Methods 1 and 2 using 10 dB dynamic range is two beams, and using Method 3 it is three. Corresponding 90 percentiles are four, six, and 14 beams. In the case of 20 dB dynamic range the number of beams inevitably increases, the median beam numbers are four and six with Methods 1 and 2, respectively.

IV. DISCUSSION

We have proposed three alternative methods to assess the number of beams that measured PADD of a sub-THz propagation channel supports. Analyzed measurement data is from large to medium size indoor environments, in LOS and OLOS propagation conditions at about 140 GHz frequency. These channels support only one beam in 11%–42% of cases. Two beams are supported in 23%–29% and three beams in 13%–23% of cases. Four or more beams can be allocated in 14%–40%, depending on the selected evaluation method.

The examples of our letter were based on unidirectional PADD measurements. If data was bidirectional we had at least two options. First, bi-directional propagation data can be always reduced to uni-directional PADD by integrating over angles of the other link end. Second, the introduced methods can be extended to bi-directional by substituting function $B_q(\alpha)$ by bivariate function $B_q(\alpha_1, \alpha_2)$, where α_1 and α_2 denote steering angles of the Rx and Tx, respectively. We expect that the number of beams in bidirectional case would increase but the quantity is left for further study.

In a practical system, the number of beams depends on the signal bandwidth and capabilities of RF transceivers including transmit power and noise. The dynamic range of radio transceivers will be typically narrower at upper mm-wave bands and at high bandwidth, and high-order modulations reduces the possible dynamic range window even further even if independent subarrays will be adopted for each beam. This supports the rather narrow dynamic range of beam powers used in this letter. An additional concern is availability of independent channels for MIMO for increased spectral efficiency that is not exactly the same concept as independent beams.

The question of the title is interesting to many who research and design antennas, beamforming, algorithms, etc. for future sub-THz communications. The main contribution of this letter is in the proposed methods to address the question. However, we gave an approximate answer with the limited data we have available. In a later phase, with more data from different environments and frequencies, a more comprehensive quantitative answer can be given.

REFERENCES

- [1] M. Latva-aho and K. Leppänen, Eds., “Key drivers and research challenges for 6G ubiquitous wireless intelligence,” White Paper, Sep. 2019.
- [2] K. Rikkinen, P. Kyösti, M. E. Leinonen, M. Berg, and A. Pärssinen, “THz radio communication: Link budget analysis toward 6G,” *IEEE Commun. Mag.*, vol. 58, no. 11, pp. 22–27, Nov. 2020.
- [3] T. Tuovinen, N. Tervo, and A. Pärssinen, “Analyzing 5G RF system performance and relation to link budget for directive MIMO,” *IEEE Trans. Antennas Propag.*, vol. 65, no. 12, pp. 6636–6645, Dec. 2017.
- [4] N. A. Abbasi *et al.*, “Double directional channel measurements for THz communications in an urban environment,” in *Proc. IEEE Int. Conf. Commun.*, 2020, pp. 1–6.
- [5] S. L. H. Nguyen, K. Haneda, J. Järveläinen, A. Karttunen, and J. Putkonen, “Comparing radio propagation channels between 28 and 140 GHz bands in a shopping mall,” in *Proc. 12th Eur. Conf. Antennas Propag. (EuCAP2018)*, 2018, pp. 1–5.
- [6] S. Ju, Y. Xing, O. Kanhere, and T. S. Rappaport, “Millimeter wave and sub-terahertz spatial statistical channel model for an indoor office building,” *IEEE J. Sel. Areas Commun.*, vol. 39, no. 6, pp. 1561–1575, Jun. 2021.
- [7] A. Poon, R. Brodersen, and D. Tse, “Degrees of freedom in multiple-antenna channels: A signal space approach,” *IEEE Trans. Inf. Theory*, vol. 51, no. 2, pp. 523–536, Feb. 2005.
- [8] M. Migliore, “On the role of the number of degrees of freedom of the field in MIMO channels,” *IEEE Trans. Antennas Propag.*, vol. 54, no. 2, pp. 620–628, Feb. 2006.
- [9] K. Haneda, S. L. Hong Nguyen, and A. Khatun, “Attainable capacity of spatial radio channels: A multiple-frequency analysis,” in *Proc. Globecom Workshop*, Wanshington, DC, USA, 2016, pp. 1–5.
- [10] A. F. Molisch *et al.*, “Hybrid beamforming for massive MIMO: A survey,” *IEEE Commun. Mag.*, vol. 55, no. 9, pp. 134–141, Sep. 2017.
- [11] W. Hong *et al.*, “mmWave 5G NR cellular handset prototype featuring optically invisible beamforming antenna-on-display,” *IEEE Commun. Mag.*, vol. 58, no. 8, pp. 54–60, Aug. 2020.
- [12] K. Haneda, C. Gustafson, and S. Wyne, “60 GHz spatial radio transmission: Multiplexing or beamforming?,” *IEEE Trans. Antennas Propag.*, vol. 61, no. 11, pp. 5735–5743, Nov. 2013.
- [13] TR 38.901, “Study on channel model for frequencies from 0.5 to 100 GHz,” 3GPP, Tech. Rep. V14.1.1, Jul. 2017.
- [14] S. L. H. Nguyen, K. Haneda, J. Järveläinen, A. Karttunen, and J. Putkonen, “Large-scale parameters of spatio-temporal short-range indoor backhaul channels at 140 GHz,” in *Proc. IEEE 93rd Veh. Technol. Conf.*, 2021, pp. 1–6.